

Quasiparticle Description of Hot QCD at Finite Quark Chemical Potential^{*)}

M.A. Thaler^a, R.A. Schneider^{a,b}, W. Weise^{a,b}

^a*Physik-Department, Technische Universität München D-85747 Garching, GERMANY*

^b*ECT*, I-38050 Villazzano (Trento), ITALY*

Abstract

We study the extension of a phenomenologically successful quasiparticle model that describes lattice results of the equation of state of the deconfined phase of QCD for $T_c \leq T \lesssim 4T_c$, to finite quark chemical potential μ . The phase boundary line $T_c(\mu)$, the pressure difference $\Delta p(T, \mu) = (p(T, \mu) - p(T, \mu = 0))/T^4$ and the quark number density $n_q(T, \mu)/T^3$ are calculated and compared to recent lattice results. Good agreement is found up to quark chemical potentials of order $\mu \sim T_c$.

^{*)}Work supported in part by BMBF and GSI

1 Introduction

The phase structure of QCD at high temperature and non-vanishing baryon chemical potential has been subject of intense research in recent years. Heavy-ion collisions at high energies have been and are being explored at SPS/CERN and RHIC/BNL [1] in search for signals of the Quark-Gluon Plasma (QGP). Large-scale lattice QCD computations at finite temperature have been performed [2, 3, 4], and first extensions to non-zero baryon chemical potential appear now to be feasible. It has proven possible to trace out the phase boundary line $T_c(\mu)$ separating the hadronic phase from the QGP phase for $N_f = 4$ [5, 6], $N_f = 2$ [7] and $N_f = 3$ [8] flavors of quarks up to quark chemical potentials μ of order T_c . First numerical results for the QCD Equation of State (EoS), i.e. the pressure $p(T, \mu)$ and the quark number density $n_q(T, \mu)$ are also available for $N_f = 2 + 1$ [9] and $N_f = 2$ [10]. As well as being of intrinsic theoretical interest, such studies provide conceptual guidance for current heavy ion collision experiments at SPS and RHIC, where the chemical freeze-out occurs at $\mu_{f.o.} \simeq 100$ MeV, (baryon chemical potential $\mu_B \simeq 300$ MeV) [11] and $\mu_{f.o.} \simeq 15$ MeV, ($\mu_B \simeq 45$ MeV) [12], respectively.

Systematic perturbative expansions of the QCD equation of state within the framework of thermal field theory show bad convergence even for very large temperatures (several times T_c) far beyond the region accessible to present experiments [13]. Various techniques, such as dimensional reduction, screened perturbation theory or hard-thermal loop (HTL) perturbation theory show better convergence and good agreement with lattice results for $T \gtrsim 3T_c$ [14]. Various interpretations of the lattice data have been attempted in terms of physical quantities, most prominently as the EoS of a gas of massive quark and gluon quasiparticles. Their thermally generated masses are based on perturbative calculations carried out in the HTL scheme [15, 16, 17]. This approach has been extended to non-vanishing quark chemical potential and good agreement with finite μ lattice calculations for $N_f = 2 + 1$ flavors has been found [18]. More recently, the QGP has also been described in terms of a condensate of Z_3 Wilson lines [19] and by more refined quasiparticle models based on the HTL-resummed entropy and (NLO) extensions thereof [20]. These models have found support from resummed perturbation theory [21] for temperatures $T \gtrsim 3T_c$. However, they have difficulties explaining the dropping of the thermal gluon screening mass in the vicinity of the phase transition. An improved quasiparticle model [22] shows the correct temperature dependence of the Debye mass and reproduces lattice thermodynamical quantities such as the pressure, the energy density and the entropy density very well. The main new ingredient of this model is a phenomenological parametrization of (de)confinement.

In the present work, this improved quasiparticle model is extended to finite quark chemical potential μ . In section 2, a brief review of the quasiparticle model with confinement is given. The extension of the model to finite quark chemical potential μ is discussed in detail in section 3. Numerical results are presented in chapter 4. The phase boundary line $T_c(\mu)$ that separates the hadronic from the QGP-phase is discussed and the quasiparticle model result is compared to recent lattice simulations. Results for the pressure difference from $\mu = 0$ and the quark number density for various values of the chemical potential μ are also presented and compared to recent lattice simulations. A summary is given in section 5.

2 Quasiparticle model with confinement

It is possible to describe the EoS of hot QCD at vanishing quark chemical potential μ to good approximation by the EoS of a gas of quasiparticles with thermally generated masses, incorporating confinement effectively by a temperature-dependent, reduced number of thermodynamically active degrees of freedom. This method is briefly outlined in this section. For a more detailed discussion the reader is referred to ref.[22].

At very high temperatures, spectral functions for gluons or quarks of the form $\delta(E^2 - k^2 - m^2(T))$ with

$m(T) \sim gT$ are found in HTL perturbative calculations. Here, E is the particle energy, k the absolute value of its momentum, $m(T)$ its thermally generated mass and g the QCD coupling constant. As long as the spectral function at lower temperatures resembles qualitatively this asymptotic form, a quasiparticle description is expected to be applicable. QCD dynamics is then incorporated in the thermal masses of the quark and gluon quasiparticles. These thermal masses are obtained from the self-energies of the corresponding particles, evaluated at thermal momenta $k \sim T$:

$$m_q^2 = m_{0q}^2 + \frac{N_c^2 - 1}{8N_c} \left(T^2 + \frac{\mu^2}{\pi^2} \right) G^2(T, \mu), \quad (1)$$

$$m_g^2 = m_{0g}^2 + \frac{1}{6} \left[\left(N_c + \frac{N_f}{2} \right) T^2 + \frac{3}{2\pi^2} \sum_q \mu_q^2 \right] G^2(T, \mu). \quad (2)$$

N_f is the number of flavors, N_c the number of colors. The effective coupling strength G is specified as

$$G(T, \mu = 0) = \frac{g_0}{\sqrt{11N_c - 2N_f}} \left([1 + \delta] - \frac{T_c}{T} \right)^\beta. \quad (3)$$

Setting $g_0 = 9.4$, $\beta = 0.1$, the effective masses as given in equations (1) and (2), approach the HTL result at high temperatures. (A small shift $\delta = 10^{-6}$ helps fine-tuning at $T \simeq T_c$). Because of the existence of a heat bath background, new partonic excitations, plasmons (longitudinal gluons) and plasminos (quark-hole excitations) are also present in the plasma. However, their spectral strengths are exponentially suppressed for hard momenta and large temperatures and consequently these states are essentially unpopulated [23]. The functional dependence of $m_q(T)$ on T is based on the conjecture that the phase transition is second order or weakly first order which suggests an almost power-like behavior $m \sim (T - T_c)^\beta$ with some critical exponent $\beta > 0$. It is assumed that the pseudocritical form of the effective coupling constant given in equation (3) also provides the correct approximate expression for the effective quark mass. This is supported by a non-perturbative dispersion relation analysis for a thermal quark interacting with the gluon condensate [24].

Close to T_c the picture of a non-interacting gas is not appropriate because the driving force of the transition, the confinement process, is not taken into account. Below T_c , the relevant degrees of freedom are pions and other hadrons. Approaching T_c from below, deconfinement sets in and the quarks and gluons are liberated, followed by a sudden increase in entropy and energy density. Conversely, when approaching the phase transition from above, the decrease in the thermodynamic quantities is not primarily caused by increasing masses of the quasiparticles, but by the reduction of the number of thermally active degrees of freedom due to the onset of confinement. For example, gluons begin to form heavy clusters (glueballs), so that the gluon density gets reduced as T_c is approached from above. This feature can be incorporated in the quasiparticle picture by modifying the number of effective degrees of freedom by a temperature dependent confinement factor $C(T)$:

$$C(T, \mu = 0) = C_0 \left([1 + \delta_c] - \frac{T_c}{T} \right). \quad (4)$$

The confinement factor is taken to be universal. The parameters C_0 , δ_c and β_c are fixed by reproducing the entropy density that results from lattice QCD thermodynamics. Since the results of lattice calculations with dynamical quarks are still dependent on the details of the simulations, C_0 , δ_c and β_c should be finetuned for different lattice calculations.

For homogeneous systems of large volume V , the Helmholtz free energy F is related to the pressure p by $F(T, V) = -p(T)V$. In the present framework of a gas of quasiparticles, its explicit expression reads

$$p(T) = \frac{\nu_g}{6\pi^2} \int_0^\infty dk C(T) f_B(E_k^g) \frac{k^4}{E_k^g} + \frac{2N_c}{3\pi^2} \sum_{i=1}^{N_f} \int_0^\infty dk C(T) f_D(E_k^i) \frac{k^4}{E_k^i} - B(T). \quad (5)$$

ν_g is the gluon degeneracy factor, $E_k^g = \sqrt{k^2 + m_g^2(T)}$ is the gluon energy, $E_k^q = \sqrt{k^2 + m_q^2(T)}$ the quark energy, $f_B(E_k^g) = (\exp((E_k^g)/T) - 1)^{-1}$ the Bose-Einstein distribution function of gluons and $f_D(E_k^q) = (\exp((E_k^q)/T) + 1)^{-1}$ the Fermi-Dirac distribution function of quarks. The energy density ϵ and the entropy density s take the form

$$\epsilon(T) = \frac{\nu_g}{2\pi^2} \int_0^\infty dk k^2 C(T) f_B(E_k^g) E_k^g + \frac{2N_c}{\pi^2} \sum_{i=1}^{N_f} \int_0^\infty dk k^2 C(T) f_D(E_k^i) E_k^i + B(T). \quad (6)$$

and

$$s(T) = \frac{\nu_g}{2\pi^2 T} \int_0^\infty dk k^2 C(T) f_B(E_k^g) \frac{\frac{4}{3}k^2 + m_g^2(T)}{E_k^g} + \frac{2N_c}{\pi^2 T} \sum_{i=1}^{N_f} \int_0^\infty dk k^2 C(T) f_D(E_k^i) \frac{\frac{4}{3}k^2 + m_q^2(T)}{E_k^i} \quad (7)$$

The function $B(T)$ is introduced to act as a background field. It is necessary in order to maintain thermodynamic consistency: p , ϵ and $s = \partial p / \partial T$ have to satisfy the Gibbs-Duhem relation $\epsilon + p = Ts = T \partial p / \partial T$. $B(T)$ basically compensates the additional T -derivatives from the temperature-dependent masses in p and thus is not an independent quantity. Since $B(T)$ adds to the energy density of the quasiparticles, it can be interpreted as the thermal vacuum energy density. The entropy density, as a measure of phase space, is unaffected by $B(T)$.

3 Finite chemical potential

The quasiparticle model reviewed in the previous section accurately reproduces lattice thermodynamical quantities such as the pressure, the energy density and the entropy density in the temperature range $T_c < T \lesssim 4T_c$ at vanishing chemical potential [22]. However, many physical questions, e.g. the structure of quark cores in massive neutron stars, the baryon contrast prior to cosmic confinement or the evolution of the baryon number in the mid-rapidity region of central heavy-ion collisions, require a detailed understanding of the EoS at non-vanishing quark chemical potential. In this section, a thermodynamically self-consistent extension of the quasiparticle model to finite quark chemical potentials is presented. Results for various observables are then computed and compared to finite μ lattice results in the next section.

At vanishing quark chemical potential, it is conjectured from asymptotic freedom that QCD undergoes a phase transition from the hadronic phase to the QGP phase. At extremely high density, cold quark matter is necessarily in the Color-Flavor-Locked (CFL) phase in which quarks of all three colors and all three flavors form cooper pairs. It is expected that this phase is separated from the hadronic phase by the color superconducting 2SC phase. For a review of the QCD phase diagram, the reader is referred to [25]. Our extension of the quasiparticle model provides a straightforward way to map the EoS at finite temperature and vanishing quark chemical potential into the $T - \mu$ plane without further assumptions. However, since this continuous mapping relies on quark and gluon quasiparticles, it cannot provide information about other possible phases with a different (quasiparticle) structure. It is therefore applicable in a limited range of not too large chemical potentials.

The pressure of an ideal gas of quark and gluon quasiparticles with effective masses depending on temperature and quark chemical potential, is given by

$$p(T, \mu) = \frac{\nu_g}{6\pi^2} \int_0^\infty dk C(T, \mu) f_B(E_k^g) \frac{k^4}{E_k^g} + \frac{N_c}{3\pi^2} \sum_{q=1}^{N_f} \int_0^\infty dk C(T, \mu) [f_D^+(E_k^q) + f_D^-(E_k^q)] \frac{k^4}{E_k^q} - B(T, \mu), \quad (8)$$

with $f_D^\pm(E_k^q) = (\exp((E_k^q \mp \mu)/T) + 1)^{-1}$. The effective coupling strength $G(T, \mu)$, the confinement factor $C(T, \mu)$ and the mean field contribution $B(T, \mu)$ now also depend on the quark chemical potential μ . $B(T, \mu)$ is calculated in appendix A. The quark number density (which is related to the baryon number density n_B by $n_q = n_B/3$) retains the ideal gas form

$$n_q(T, \mu) = \frac{N_c}{\pi^2} \sum_{q=1}^{N_f} \int_0^\infty dk C(T, \mu) [f_D^+(E_k^q) - f_D^-(E_k^q)] k^2, \quad (9)$$

but with the confinement factor $C(T, \mu)$ included.

In the previous section expressions for the coupling $G(T, \mu = 0)$ and the confinement factor $C(T, \mu = 0)$ are given. These expressions can be generalized to finite chemical potential in a thermodynamically self-consistent way using Maxwell relations. Imposing the Maxwell relation between the derivatives of the quark number density and the entropy,

$$\left. \frac{\partial s}{\partial \mu} \right|_T = \left. \frac{\partial n}{\partial T} \right|_\mu \implies \sum_i \left(\frac{\partial n}{\partial m_i^2} \frac{\partial m_i^2}{\partial T} - \frac{\partial s}{\partial m_i^2} \frac{\partial m_i^2}{\partial \mu} \right) = 0 \quad \text{and} \quad \left(\frac{\partial n}{\partial C} \frac{\partial C}{\partial T} - \frac{\partial s}{\partial C} \frac{\partial C}{\partial \mu} \right) = 0, \quad (10)$$

yields a set of first order quasilinear partial differential equations for the effective coupling constant $G^2(T, \mu)$ and the confinement factor $C(T, \mu)$:

$$a_T(T, \mu; G^2) \frac{\partial G^2}{\partial T} + a_\mu(T, \mu; G^2) \frac{\partial G^2}{\partial \mu} = b(T, \mu; G^2), \quad (11)$$

$$c_T(T, \mu; G^2) \frac{\partial C}{\partial T} + c_\mu(T, \mu; G^2) \frac{\partial C}{\partial \mu} = 0. \quad (12)$$

The coefficients $a_T, a_\mu, b, c_T, c_\mu$ depend on T, μ, G^2 but not on C . It can be solved by the method of characteristics (see appendix B). The flow of the effective coupling and the confinement factor is elliptic. In particular, one finds

$$a_T(T, \mu = 0) = 0, \quad a_\mu(T = 0, \mu) = 0, \quad c_T(T, \mu = 0) = 0, \quad c_\mu(T = 0, \mu) = 0. \quad (13)$$

Therefore, the characteristics are perpendicular to both the T and the μ axis. This guarantees that specifying the coupling constant and the confinement factor on the T axis sets up a valid initial condition problem. Plots of the characteristic curves and the confinement factor are shown in figure 1 and 2.

4 Comparison with lattice results

Simulations of QCD at finite chemical potential are extremely difficult because the fermion determinant becomes complex. This prohibits Monte Carlo importance sampling, which interprets the measure as a probability factor and thus requires it to be positive. While this problem remains unsolved, there are some approaches which circumvent the sign problem and allow lattice simulations for small chemical potentials $\mu \lesssim T_c$. A review comparing these methods in detail can be found in [26].

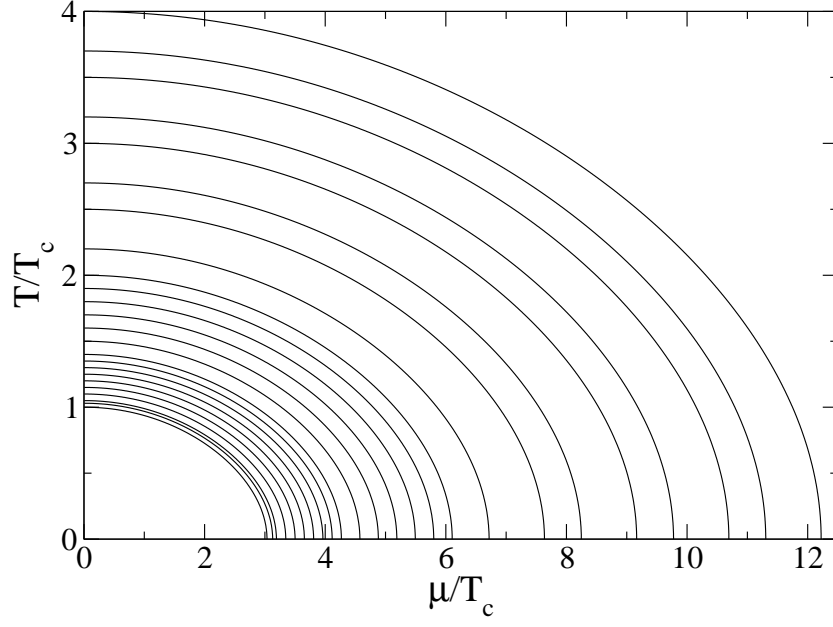


Figure 1: Characteristic curves of constant confinement factor $C(T, \mu) = \text{const}$, obtained when solving eq.(12).

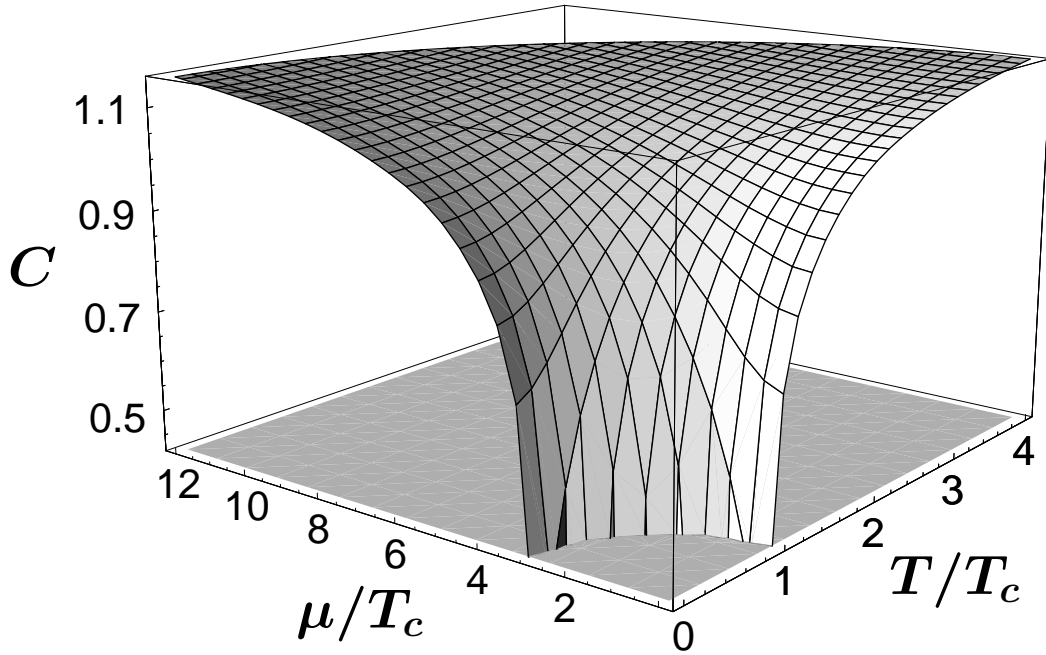


Figure 2: The confinement factor $C(T, \mu)$ as a function of the temperature T and the quark chemical potential μ .

4.1 The phase boundary line

In the case of vanishing chemical potential, universal arguments and lattice simulations suggest a phase transition from the hadronic phase to the QGP phase at a critical temperature T_c . For QCD with three light flavors $m_u \sim m_d \sim m_s \sim 5$ MeV this transition is expected to be first order. For two light flavors $m_u \sim m_d \sim 5$ MeV and an infinitely large m_s there is no phase transition, only a smooth crossover [27]. This suggests there is a critical strange mass m_s^c at which one finds a second order phase transition. Lattice calculations indicate that m_s^c is about half of the physical mass m_s . At finite quark chemical potential μ and vanishing T a first order phase transition is predicted. For the physical m_s this implies that there is a first order phase transition for small T and large μ which ends at a critical point (T^*, μ^*) . At this point the phase transition is of second order. For large T and small μ the two phases are separated by a crossover. We refer to the line $T_c(\mu)$ that separates the hadronic phase from the QGP phase as the “phase boundary line”. In the literature [6, 7, 8] this line is also frequently called the “pseudocritical line”. $T_c(\mu)$ has been calculated on the lattice for $N_f = 4$ [5, 6], $N_f = 2$ [7] and $N_f = 3$ [8] flavors of quarks up to quark chemical potentials μ of order T_c . In the following we focus on the three-flavor results where the critical line has been calculated with an accuracy up to terms of order $(\mu/T)^6$. There, a Wilson gauge action and three degenerate flavors of staggered quarks have been employed, with bare masses in the range $0.025 < am < 0.04$, where a denotes the lattice spacing. The finite volume scaling behavior was monitored by using three lattice sizes, $8^3 \times 4$, $10^3 \times 4$ and $12^3 \times 4$.

In our quasiparticle model, the sudden decrease of the pressure, the energy density, the quark number density and the entropy density caused by gluons and quarks getting trapped in glueballs and hadrons when T_c is approached from above, is parametrized by the confinement factor $C(T, \mu)$. Consequently, it is natural to relate the critical line to the characteristic curve of the confinement factor through $T_c(\mu)$, as long as μ is small and the nature of the quasiparticles does not change qualitatively.

In order to calculate the confinement factor at finite chemical potential, we need to specify a valid initial condition, e.g. $C(T, \mu = 0)$. The functional form of $C(T, \mu = 0)$ is set by eq.(4). We have employed the following set of parameters, as found in ref.[22]:

	C_0	δ_c	β_c
3 flavors	1.03	0.02	0.2

We have checked that the form of the phase boundary line in the quasiparticle model depends only weakly on the exact choice of parameters and a small difference only shows up for values much larger than the range of μ covered by the lattice simulations. The lattice phase boundary line and our result is shown in figure 3. The quasiparticle result is within the lattice estimate for $\mu_B \lesssim 2.5T_c$ and deviates only slightly from the lattice result for larger chemical potentials.

4.2 Thermodynamical quantities

There have been lattice calculations of thermodynamical quantities at finite chemical potential for $N_f = 2 + 1$ [9] and $N_f = 2$ [10] flavors of quarks. In the following we focus on results from [10] where a p4-improved staggered action on a $16^3 \times 4$ lattice was used. There, the N_τ dependence is known to be small, in contrast to standard staggered fermion actions which show substantially larger cut-off effects. Estimates of the pressure, the quark number density and associated susceptibilities as functions of the quark chemical potential were made via a Taylor series expansion of the thermodynamic grand canonical potential Ω up to fourth order.

To calculate thermodynamical quantities within the quasiparticle model, we need to fix the parameters of the effective coupling constant and the confinement factor. Our calculations have shown that the results are not sensitive to the detailed choice of parameters for the effective coupling G . We have therefore used

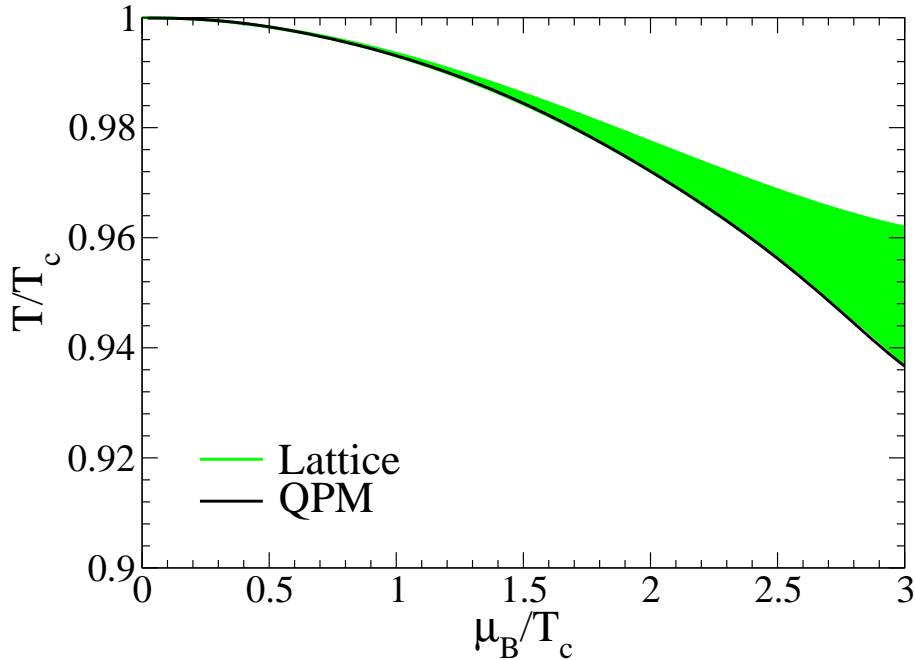


Figure 3: The phase boundary line $T_c(\mu)$ calculated with the quasiparticle model for $N_f = 3$. The shaded band shows the one-sigma error band obtained in lattice calculations in [8].

the parameters from ref.[22] in our calculations. In principle, the parameters of the confinement factor can be fixed by comparing our calculations to lattice results at vanishing chemical potential. However, in ref.[10] no $\mu = 0$ lattice data is given. Since lattice calculations including quarks give slightly different results depending on which action has been used, fitting the parameters in $C(T, \mu = 0)$ by comparing quasiparticle results to lattice data from a different simulation is not feasible and would lead to large differences. Consequently, we directly used the finite μ lattice results for fitting. Good agreement with the lattice thermodynamical observables was found for the following sets of parameters:

	C_0	δ_c	β_c
Set A	1.05	-0.016	0.15
Set B	1.12	0.02	0.2

While set A reproduces the lattice thermodynamical results slightly better, set B is in better agreement with the parameters found in [22] for $\mu = 0$ lattice simulations.

The temperature dependence of the normalized pressure difference $\Delta p(T, \mu) = (p(T, \mu) - p(T, \mu = 0))/T^4$ is shown in figure 4 and that of the normalized quark number density $n_q(T, \mu)/T^3$ in figure 5. Whereas the computation of the quark number density from equation (9) is straightforward, a numerical evaluation of (8) is difficult because of the derivatives of the effective masses and the confinement factor in $B(T, \mu)$ (see expressions in appendix A). It turns out that it is simpler to calculate the pressure difference using the following relation:

$$\Delta p(T, \mu) = \frac{1}{T^4} \int_0^\mu d\mu' n_q(T, \mu'). \quad (14)$$

The lattice pressure difference is well reproduced even for the largest values of the chemical potential. The quark number density is in very good agreement with the lattice data for $\mu/T_c = 0.2$ and 0.4. For

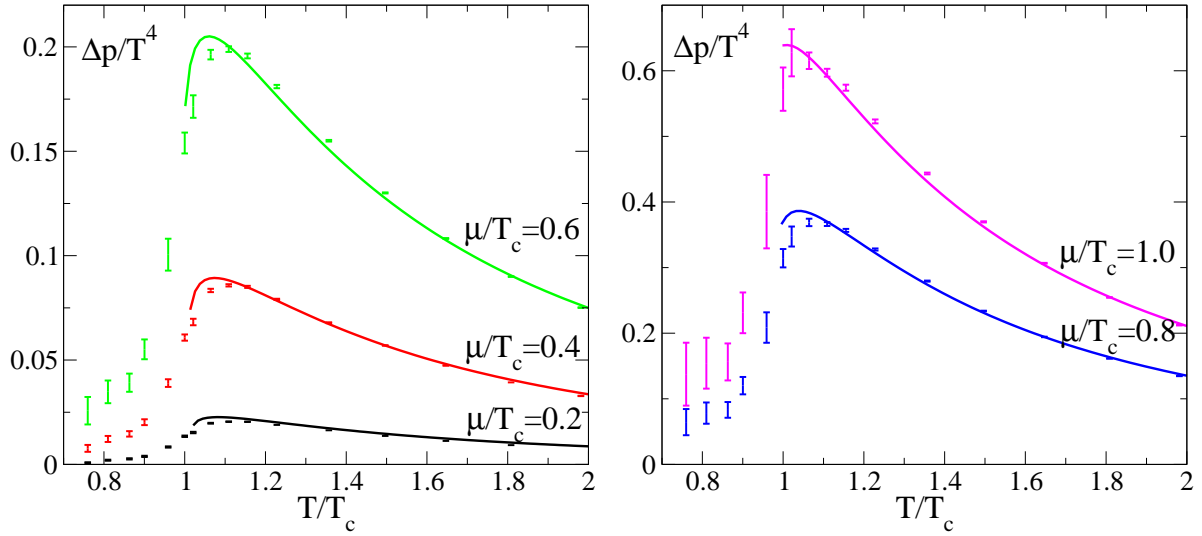


Figure 4: The normalized pressure difference $\Delta p(T, \mu)/T^4$ as a function of temperature compared to lattice results from [10] (symbols).

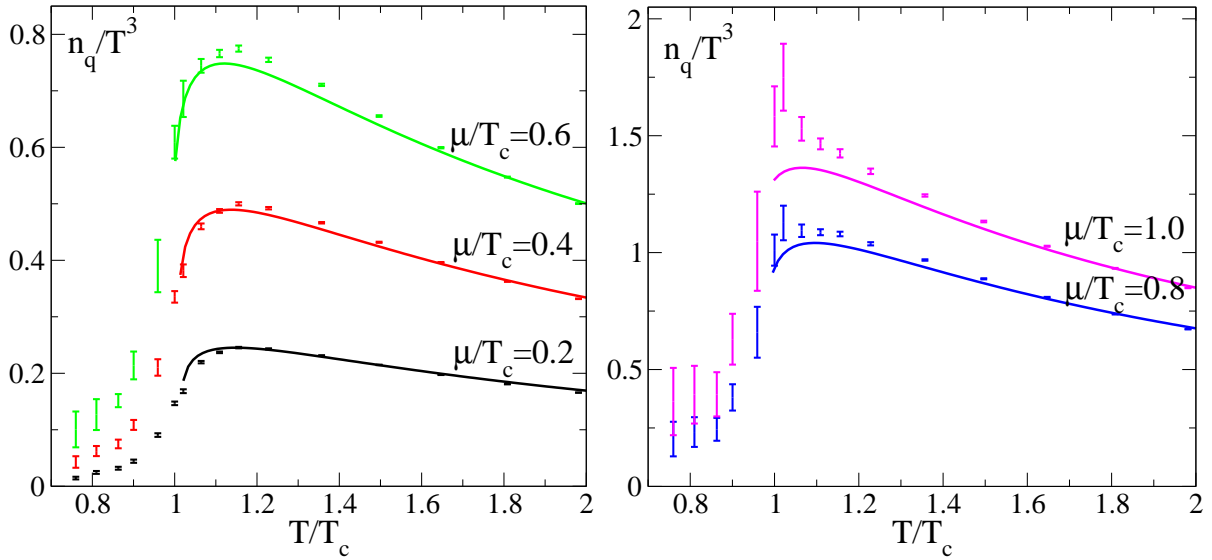


Figure 5: The normalized quark number density $n_q(T, \mu)/T^3$ as a function of temperature compared to lattice results from [10] (symbols).

larger values of μ our calculations underestimate the magnitude of the lattice results close to T_c , but show the same qualitative features.

5 Summary

We have presented a quasiparticle description of the QCD EoS at finite temperature and quark chemical potential. Our main modification as compared to previous work is the inclusion of finite quark chemical potential in a thermodynamically consistent way. We have first reviewed our improved quasiparticle model which schematically includes confinement. We have shown how Maxwell relations can be used to construct the effective coupling $G(T, \mu)$ and the confinement factor $C(T, \mu)$ at finite chemical potential. We then used this model to calculate the phase boundary line $T_c(\mu)$ and the normalized pressure difference $\Delta p(T, \mu) = (p(T, \mu) - p(T, \mu = 0))/T^4$ and the normalized quark number density $n_q(T, \mu)/T^3$. We compared our results to recent lattice calculations and found remarkably good agreement even for large quark chemical potentials $\mu \sim T_c$.

A Calculation of $B(T, \mu)$

The ‘‘background field’’ quantity $B(T, \mu)$ appearing in eq.(8) can be obtained from the Gibbs-Duhem relation

$$\epsilon + p = Ts + \mu n = T \frac{\partial p}{\partial T} + \mu \frac{\partial p}{\partial \mu}. \quad (15)$$

The left hand side reads:

$$\epsilon + p = \frac{N_c N_f}{3\pi^2} \int_0^\infty dk [f_D^+ + f_D^-] C(T, \mu) k^2 \left(\frac{4k^2 + 3m_q^2}{E_k} \right). \quad (16)$$

To evaluate the right-hand side, derivatives of $f_D^\pm(E_k^q)$ with respect to T and μ are rewritten as derivatives with respect to k . After an integration by parts, the first term on the right-hand side reads

$$\begin{aligned} T \frac{\partial p}{\partial T} &= T \frac{N_c N_f}{3\pi^2} \int_0^\infty dk f_D^+ \left(\frac{\partial C}{\partial T} \frac{k^4}{E_k} - C(T, \mu) \frac{3k^2}{2E_k} \frac{\partial m_q^2}{\partial T} + C(T, \mu)(E_k + \mu) + C(T, \mu) \frac{k^4}{TE_k} \right) \\ &+ T \frac{N_c N_f}{3\pi^2} \int_0^\infty dk f_D^- \left(\frac{\partial C}{\partial T} \frac{k^4}{E_k} - C(T, \mu) \frac{3k^2}{2E_k} \frac{\partial m_q^2}{\partial T} + C(T, \mu)(E_k - \mu) + C(T, \mu) \frac{k^4}{TE_k} \right) \\ &- T \frac{\partial B(T, \mu)}{\partial T}, \end{aligned} \quad (17)$$

and the second term is given by

$$\begin{aligned} \mu \frac{\partial p}{\partial \mu} &= \mu \frac{N_c N_f}{3\pi^2} \int_0^\infty dk f_D^+ \left(\frac{\partial C(T, \mu)}{\partial \mu} \frac{k^4}{E_k} - C(T, \mu) \frac{\partial m_q^2}{\partial \mu} \frac{3k^2}{2E_k} - C(T, \mu) 3k^2 \right) \\ &+ \mu \frac{N_c N_f}{3\pi^2} \int_0^\infty dk f_D^- \left(\frac{\partial C(T, \mu)}{\partial \mu} \frac{k^4}{E_k} - C(T, \mu) \frac{\partial m_q^2}{\partial \mu} \frac{3k^2}{2E_k} + C(T, \mu) 3k^2 \right) - \mu \frac{\partial B(T, \mu)}{\partial \mu}. \end{aligned} \quad (18)$$

Substituting (16), (17) and (18) in the Gibbs-Duhem relation yields a partial differential equation of the type

$$x \frac{\partial f(x, y)}{\partial x} + y \frac{\partial f(x, y)}{\partial y} = \mathcal{I}(x, y). \quad (19)$$

It has the general solution

$$f(x, y) = \int^x dt \mathcal{I}(t, \frac{y}{x}) + \mathcal{H}\left(\frac{y}{x}\right). \quad (20)$$

Here, $\mathcal{H}(y/x)$ is a solution of the homogeneous equation. Returning to our case, $\mathcal{H}(\mu/T)$ becomes an arbitrary function of the ratio μ/T to be fixed by boundary conditions. For $\mu \rightarrow 0$, $\mathcal{H}(\mu/T)$ does not depend on T anymore and therefore has to be identified with an integration constant B_0 . Provided that $\mathcal{H}(\mu/T)$ is a continuous function it must be close to B_0 for small μ/T . The first term in a Taylor expansion of $\mathcal{H}(\mu/T)$ vanishes and the series starts only at order $(\mu/T)^2$. Therefore we identify $\mathcal{H}(\mu/T)$ with the constant B_0 for all μ under consideration. Assembling all pieces, the final result reads

$$\begin{aligned} B(T, \mu) &= B_1(T, \mu) + B_2(T, \mu) + B_0, \\ B_1(T, \mu) &= \frac{N_c N_f}{3\pi^2} \int_0^\infty dk \int_{T_c}^T d\tau [f_D^+(E_k^q) + f_D^-(E_k^q)] \left(\frac{\partial C}{\partial \tau} + \frac{\mu}{T} \frac{\partial C}{\partial (\frac{\mu}{T}\tau)} \right) \frac{k^4}{E_k^q}, \\ B_2(T, \mu) &= -\frac{N_c N_f}{2\pi^2} \int_0^\infty dk \int_{T_c}^T d\tau C [f_D^+(E_k^q) + f_D^-(E_k^q)] \left(\frac{\partial m_q^2}{\partial \tau} + \frac{\mu}{T} \frac{\partial m_q^2}{\partial (\frac{\mu}{T}\tau)} \right) \frac{k^2}{E_k^q}, \end{aligned} \quad (21)$$

where the explicit τ -dependence in $C(\tau, \mu/T \tau)$, $m_q(\tau, \mu/T \tau)$ and $E_k^q(\tau, \mu/T \tau)$ has been suppressed for the sake of lucidity.

B Method of characteristics

Equations (11) and (12) are a set of coupled quasilinear first order partial differential equations for the effective coupling constant $G^2(T, \mu)$ and the confinement factor $C(T, \mu)$. Equation (11) does not depend on $C(T, \mu)$. Thus we can first solve this equation for $G^2(T, \mu)$ and insert the result in equation (12).

The usual method found in textbooks is to reduce a quasilinear partial differential equation of the form

$$a_T(T, \mu; X) \frac{\partial X}{\partial T} + a_\mu(T, \mu; X) \frac{\partial X}{\partial \mu} = c(T, \mu; X) \quad (22)$$

to a system of coupled ordinary differential equations,

$$\frac{dT(s)}{ds} = a_T, \quad \frac{d\mu(s)}{ds} = a_\mu, \quad \frac{dX(s)}{ds} = c. \quad (23)$$

This determines the characteristic curves $T(s)$, $\mu(s)$, and the evolution of X along such a curve, given an initial value. However, this method is not well suited for numerical use which is necessary for non-trivial a_T , a_μ and c . Rewriting equation (22) as

$$a_T \left(\frac{dX}{dT} - \frac{\partial X}{\partial \mu} \frac{d\mu}{dT} \right) + a_\mu \frac{\partial X}{\partial \mu} = c \implies \frac{\partial X}{\partial \mu} \left(a_\mu dT - d\mu \right) = \frac{c}{a_T} dT - dX, \quad (24)$$

we find the equation $a_\mu dT - a_T d\mu = 0$ for the characteristics and $cdT - a_T dX = 0$ for the evolution of X . These equations can easily be solved numerically.

References

- [1] U. W. Heinz, arXiv:nucl-th/0212004.
- [2] S. Gottlieb *et al.*, Phys. Rev. D **55**, 6852 (1997).
- [3] F. Karsch, E. Laermann and A. Peikert, Phys. Lett. B **478**, 447 (2000).

- [4] A. Ali Khan *et al.* [CP-PACS collaboration], Phys. Rev. D **64**, 074510 (2001).
- [5] Z. Fodor and S. D. Katz, Phys. Lett. B **534**, 87 (2002).
- [6] M. D'Elia and M. P. Lombardo, Phys. Rev. D **67**, 014505 (2003).
- [7] P. de Forcrand and O. Philipsen, Nucl. Phys. B **642**, 290 (2002).
- [8] P. de Forcrand and O. Philipsen, arXiv:hep-lat/0307020.
- [9] Z. Fodor, S. D. Katz and K. K. Szabo, arXiv:hep-lat/0208078.
- [10] C. R. Allton, S. Ejiri, S. J. Hands, O. Kaczmarek, F. Karsch, E. Laermann and C. Schmidt, Phys. Rev. D **68**, 014507 (2003).
- [11] P. Braun-Munzinger, I. Heppe and J. Stachel, Phys. Lett. B **465**, 15 (1999).
- [12] P. Braun-Munzinger, D. Magestro, K. Redlich and J. Stachel, Phys. Lett. B **518**, 41 (2001).
- [13] K. Kajantie, M. Laine, K. Rummukainen and Y. Schroder, arXiv:hep-ph/0211321.
- [14] J. P. Blaizot, E. Iancu and A. Rebhan, arXiv:hep-ph/0303185.
- [15] A. Peshier, B. Kämpfer, O. P. Pavlenko and G. Soff, Phys. Rev. D **54**, 2399 (1996).
- [16] P. Levai and U. W. Heinz, Phys. Rev. C **57**, 1879 (1998).
- [17] A. Peshier, B. Kämpfer and G. Soff, Phys. Rev. C **61**, 045203 (2000).
- [18] K. K. Szabo and A. I. Toth, JHEP **0306**, 008 (2003).
- [19] R. D. Pisarski, Phys. Rev. D **62**, 111501 (2000).
- [20] A. Rebhan and P. Romatschke, Phys. Rev. D **68**, 025022 (2003).
- [21] J. P. Blaizot and E. Iancu, Phys. Rept. **359**, 355 (2002).
- [22] R. A. Schneider and W. Weise, Phys. Rev. C **64**, 055201 (2001).
- [23] M. Le Bellac, *Thermal Field Theory*, Cambridge University Press, Cambridge (1996).
- [24] A. Schaefer and M. H. Thoma, Phys. Lett. B **451**, 195 (1999).
- [25] K. Rajagopal, Nucl. Phys. A **661**, 150 (1999).
- [26] E. Laermann and O. Philipsen, arXiv:hep-ph/0303042.
- [27] Z. Fodor and S. D. Katz, JHEP **0203**, 014 (2002).
- [28] K. Rajagopal and F. Wilczek, arXiv:hep-ph/0011333.